Electronic Supplementary Material (ESI) for Environmental Science: Nano.

Supporting info for:
Sludge concentration, shear rate and nanoparticle size determine silver nanoparticle removal during wastewater treatment

Cornelis, G.[1,2]; Forsberg-Grivogiannis[2], A.M.; Sköld[2], N.P.; Rauch, S.[3]; Perez-Holmberg, J.[2,]

[1] Swedish University of Agricultural Sciences, Dept. Soil and Environment, Lennart Hjelms Väg 9, 75651 Uppsala, Sweden.
[2] Gothenburg University, Dept. Chemistry and molecular Biology, Kemivägen 10, 41296 Göteborg, Sweden.
[3] Water Environment Technology, Department of Civil and Environmental Engineering, Chalmers University of Technology, 41296 Göteborg, Sweden.

Contents

Sludge particle size distribution 2
Experimental method development 2
Homoaggregation 2
Recovery during filtration 2
Filtration versus centrifugation 3
Filtration of ME 4
Optimal total Ag concentration 5
Experimental conditions during batch and sedimentation tests 6
Attachment kinetic data 8
Attachment and detachment rate calculation 9
Additional sedimentation experiments 12
Literature meta-analysis 13
Literature data 13
Additional ENP properties 21
Results 22
References 23

Sludge particle size distribution

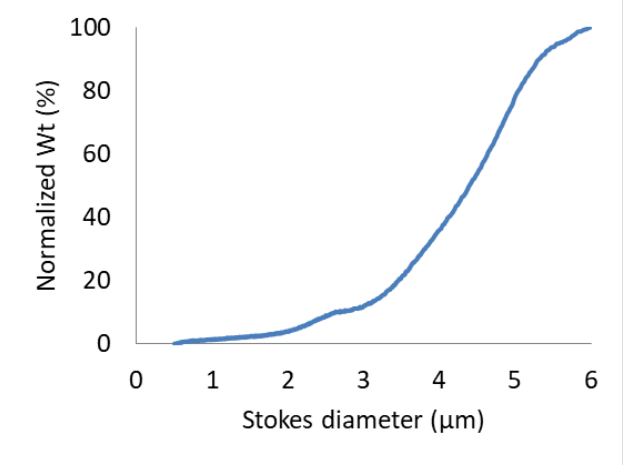

Figure S1. Mass based Stokes diameter distribution of sludge particles measured using differential centrifugal sedimentation analysis. The mass is relative to the highest calculated mass. Mass was calculated from light scattering using Mie theory and a refractive index of 1.52 and an absorption coefficient 1.0.1

Experimental method development

Homoaggregation

Recovery during filtration could be limited because of homo aggregation of Ag ENPs, which would lead to overestimation of the attachment rate of AgNP to AS flocs. This was analysed by adding 500 µL BBI (5 mg L^{-1}; nominal size 80 nm) to 3 mL of 10 kDa filtered activated sludge liquor (ASQ) and measuring the Z-average hydrodynamic diameter at 24 h, 48 h and after 1 week using a Malvern Zetasizer.

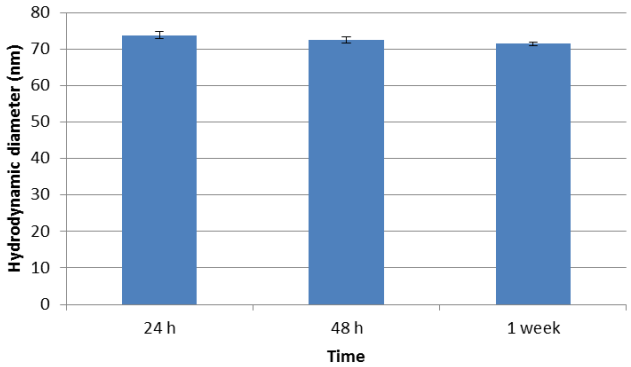

Figure S2 Staple diagram showing how the size of citrate coated Ag-NPs (normal size 80 nm) in 1-kDa filtrate of MLQ changes over time.

The DLS results, seen in figure 6, showed that the NP size is rather constant over time, excluding homo-aggregation as an issue for the filter recovery.

Recovery during filtration

Three membrane types of 0.45 µm filter materials were compared: cellulose triacetate (CTA, Sartorius) and poly vinylidene fluoride (PVDF, Sartorius) and hydrophilic polyether sulfone (PES, Supor). Three parallel comparisons were made by diluting 187 µL of Ag-NP stock solution (5 ppm; nominal size 80 nm) in 50 mL of 10-kDa filtered ME for each comparison and followed by

homogenisation for 15 seconds in a vortex shaker at 3000 rpm. The recovery was determined by comparing three replicates of each filter type (CTA, PVDF and PES) with the untreated solution of 10 kDa filtrate and Ag-NP. All samples were directly acidified to 1 % with concentrated HNO_3 and then measured with ICP-MS (limit of detection (LOD) = 3 ng L^{-1}).

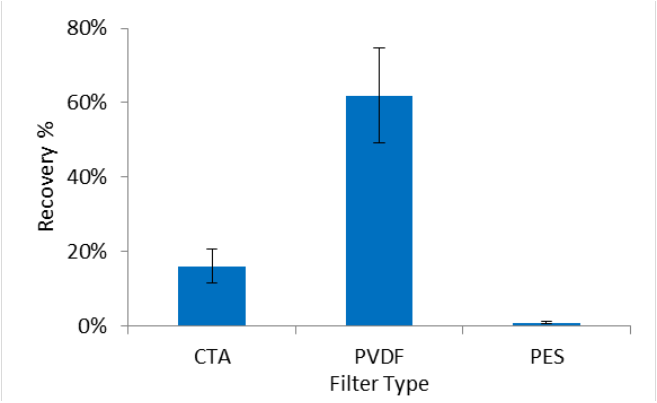

Figure S3. Recovery of Ag ENPs in 10 kDa filtrate of ME for three 0.45 µm filter types; cellulose triacetate (CTA), poly vinylidene fluoride (PVDF) and hydrophilic polyether sulfone (PES).

The results seen in Figure S3 clearly show that the filter membrane has an effect on the recovery of Ag NP, where the PVDF filters showed most promising results. However, the recovery was still only 60 %. Centrifugation was therefore considered as an alternative.

Filtration versus centrifugation

50-µL aliquots of Ag-NP stock solution (5 ppm; nominal size 80 nm) were diluted in two solutions of 50-mL 10-kDa filtrate each, and homogenised in a vortex shaker at 3000 rpm for 15 seconds. The spiked concentration was thus 5 µg L^{-1}, lower than in the previous experiment. The reason was that measured concentrations during that experiment were found to be well above the limit of detection and 5 µg L^{-1} was considered a more realistic concentration for an actual WWT.

Six 5-µg L^{-1} Ag ENP suspensions were thus 0.45-µm PVDF-filtered, three replicates were centrifuged at 4400 rpm for 2 minutes and three at 5 minutes at the same time. Filtrates, supernatants and three untreated controls were then sampled and acidified up to 2 % HNO3. The acidification was increased to 2 % (relative to 1 % in the previous experiment) to reassure that all Ag-NPs were dissolved to Ag^+ before measurement with ICP-MS. A 500 µL aliquot from each sample was also digested, to see if it would improve recovery, using the method described in the main text.

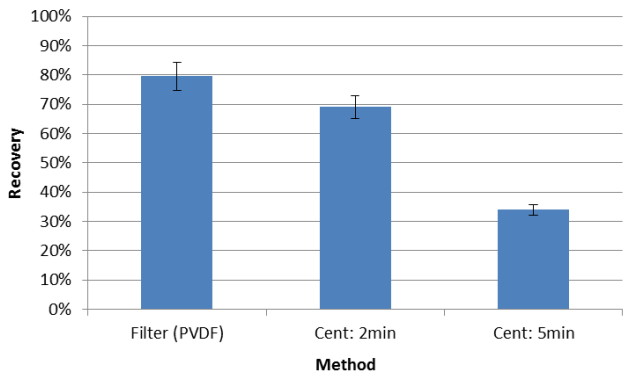

Figure S4 Recovery of Ag ENPs relative to digested controls using three different methods: 0.45 µm PVDF filters and 2 and 5 minute centrifugation at 4400 rpm.

Figure S4 shows that PVDF filtration resulted in a better recovery compared to centrifugation. Moreover, comparison between digested and undigested samples showed a 22 ± 6 % lower recovery for undigested samples. There was thus almost a 100 % recovery during PVDF filtration, a 40 % increase in recovery relative to the previous experiment (Figure S3), an increase that probably owes to using 2 % HNO3 instead of only 1 % in the previous experiment. Filtration was therefore preferred, even more because filtration occurs much faster than centrifugation. The latter technique is incompatible with the fast attachment kinetics of ENP with sludge. During centrifugation, ENP continue attaching to AS sludge.

20 % loss because of not digesting was considered acceptable as digestion introduces multiple extra error-prone methodical steps. Moreover, a dilution is required to reduce the acid concentration to a level acceptable for ICP-MS measurement (3 %). Such a dilution step increases the detection limits of the method. To minimize errors because of not digesting, 10 kDa controls that were not digested either were run for all experiments.

Filtration of ME

ME was filtered 10 kDa at all times to achieve a suspension free of "large flocs". A 10 kDa may seem rather arbitrary as it still contains flocs, albeit rather small ones. The effect of the filter cut-off on recovery during 0.45-µm filtration was investigated by passing the 10 kDa filtrate through an additional 2-kDa cross-flow membrane (Sartorius Vivaflow 200). A 50 µL aliquot of Ag ENP stock solution (5 ppm; nominal size 80 nm) was added to 50 mL of 10-kDa or 2-kDa medium and then homogenised in a vortex shaker at 3000 rpm for 15 seconds. Six replicates of each medium were passed through a PVDF filter and compared against three replicates of untreated filtrate. All samples were acidified to 2 % with concentrated HNO_3 before being measured with the ICP-MS.

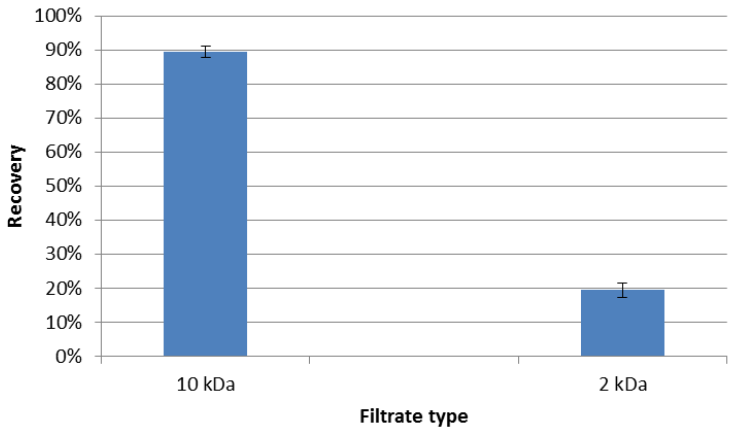

Figure S5 Recovery of Ag ENPs in two different solution media of ultrafiltrated ME; filtrate from a 10- and 2-kDa membrane.

Figure S5 shows that recovery was significantly better for Ag ENPs suspended in 10 kDa filtered ME. One possible explanation is increased steric repulsion between Ag ENP and membrane surface both coated with larger 10-kDa suspended organic compounds [2]. 10 kDa can thus be considered a medium much more representative of a floc-free medium as a 2 kDa medium. Using a 2 kDa medium instead would reduce the Ag concentration in filtrates not because of attachment, but because of attachment to filters and attachment rates would thus be overestimated.

Optimal total Ag concentration

The method was tested on three replicates of 5 µg L^{-1} Ag-NP spiked into 400 mL ME, one replicate of 50 µg L^{-1} Ag-NP spiked into 400 mL ME. A control solution of 5 µg L^{-1} Ag NP spiked into 400 mL 10 kDa filtrate was also run. The solutions were homogenised for 10 min at 200 rpm in the flocculator, prior to spiking with 400 µL (respectively 4000 µL for the 50 ppb solution) of Ag-NP stock (5 ppm; nominal size 80 nm) to all beakers. Samples were then collected at four time intervals (0 – 15, 15 – 30 and 30 – 45 min and 18 h) and filtered through a 0.45 µm PVDF filter. All samples were directly acidified to 2 % with concentrated HNO_3 and measured with ICP-MS the day after. The amount of attached Ag-NPs to the sludge (retention) was calculated using equation 1.

$$R = 1 - \frac{[Ag]_{ME}}{[Ag]_{UF}} \qquad Eq.\ 1$$

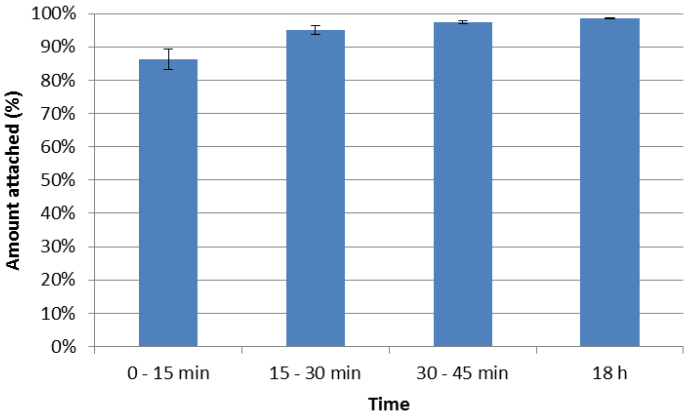

Figure S6 Staple diagram showing the amount of attached Ag-NPs to wastewater sludge over time after initial 5 ppb spiking at 200 rpm

Only results for 5 µg L^{-1} Ag-NP total concentrations are shown in Figure S6 because this concentration was clearly high enough to detect attachment, because measured concentrations were at least four times higher than the limit of detection (3 ng L^{-1}) .

Based on the results seen in figures 6 –10 the selected method of choice was to use the 0.45 µm PVDF filters to separate sludge, and thus any sludge-attached Ag NPs, from unattached Ag NPs. The loss of Ag due to direct deposition on the membrane is assumed to be low as the fraction of the unattached Ag-NPs is expected to decrease over time. The spiking concentration of the samples was chosen to be 5 µg L^{-1} of Ag-NP and an untreated (i.e. not to be passed through the PVDF filters) solution of Ag-NPs and 10 kDa filtrate was used as a reference solution. Eight time points (20 seconds, 2, 5, 15, 30, 60, 120 & 240 minutes) were selected for collecting samples ranging from the shortest of 20 seconds, a time considered minimally required to homogenise the samples, to 240 minutes, the residence time of the activated sludge tank [3].

Experimental conditions during batch and sedimentation tests

Table S1. Overview of experimental conditions during batch tests

Particle	[AS] ($g\ L^{-1}$)	Rotation rate (rpm)	pH	EC ($\mu S\ cm^{-1}$)	Attachment rate x 10^9 (s^{-1})	Detachment rate x 10^4 (s^{-1})	X ($L\ g^{-1}$)
80 nm - citrate	3.04	200	6.88	874	16	1.8	31
80 nm - citrate	2.28	200	6.88	874	11	1.5	57
80 nm - citrate	2.01	200	6.88	874	6.5	2.1	28
80 nm - citrate	1.52	200	6.88	874	8.3	4.2	37
80 nm - citrate	0.91	200	6.88	874	8.0	5.1	47
80 nm - citrate	2.62	100	7.06	780	5.0	7.1	2.7
80 nm - citrate	1.83	100	7.06	780	7.1	5.3	7.1
80 nm - citrate	0.79	100	7.06	780	4.9	22.4	4.5
80 nm - citrate	0.52	100	7.06	780	2.1	5.8	7.0
80 nm - citrate	3.04	25	6.88	874	6.2	11	1.8
80 nm - citrate	2.28	25	6.88	874	2.5	4.9	2.3
80 nm - citrate	2.01	25	6.88	874	2.5	1.5	8.1
80 nm - citrate	1.52	25	6.88	874	16	5.6	18
80 nm - citrate	0.91	25	6.88	874	18	8.4	24
80 nm - citrate	3.00	200	7.06	780	1.3	0.25	18
28 nm – citrate	3.00	200	7.06	780	1.5	2.3	2
80 nm - PEG	3.00	200	7.06	780	4.3	1.4	10

Table S2. Overview of experimental conditions during sedimentation tests

Particle	[AS] (g L^{-1})	NaCl (mol L^{-1})	pH	EC ($\mu S\ cm^{-1}$)
28 nm –citrate	1.4	0	6.94	764
28 nm –citrate	2.8	0	6.94	764
28 nm –citrate	5.6	0	6.94	764
28 nm –citrate	1.5	0	6.57	853
28 nm –citrate	3.0	0	6.57	853
28 nm –citrate	6.0	0	6.57	853
80 nm – citrate	1.4	0	6.94	764
80 nm – citrate	2.8	0	6.94	764
80 nm – citrate	5.6	0	6.94	764
80 nm – citrate	1.5	0	6.57	853
80 nm – citrate	3.0	0	6.57	853
80 nm – citrate	6.0	0	6.57	853
80 nm – PEG	1.4	0	6.94	764
80 nm – PEG	2.8	0	6.94	764
80 nm – PEG	5.6	0	6.94	764
80 nm – PEG	1.5	0	6.57	853
80 nm - PEG	3.0	0	6.57	853
80 nm - PEG	6.0	0	6.57	853
80 nm – citrate	1.81	0	6.89	622
80 nm – citrate	1.84	0.005	6.89	1143
80 nm – citrate	1.92	0.011	6.89	1778
80 nm – citrate	1.92	0.014	6.89	2060

Attachment kinetic data

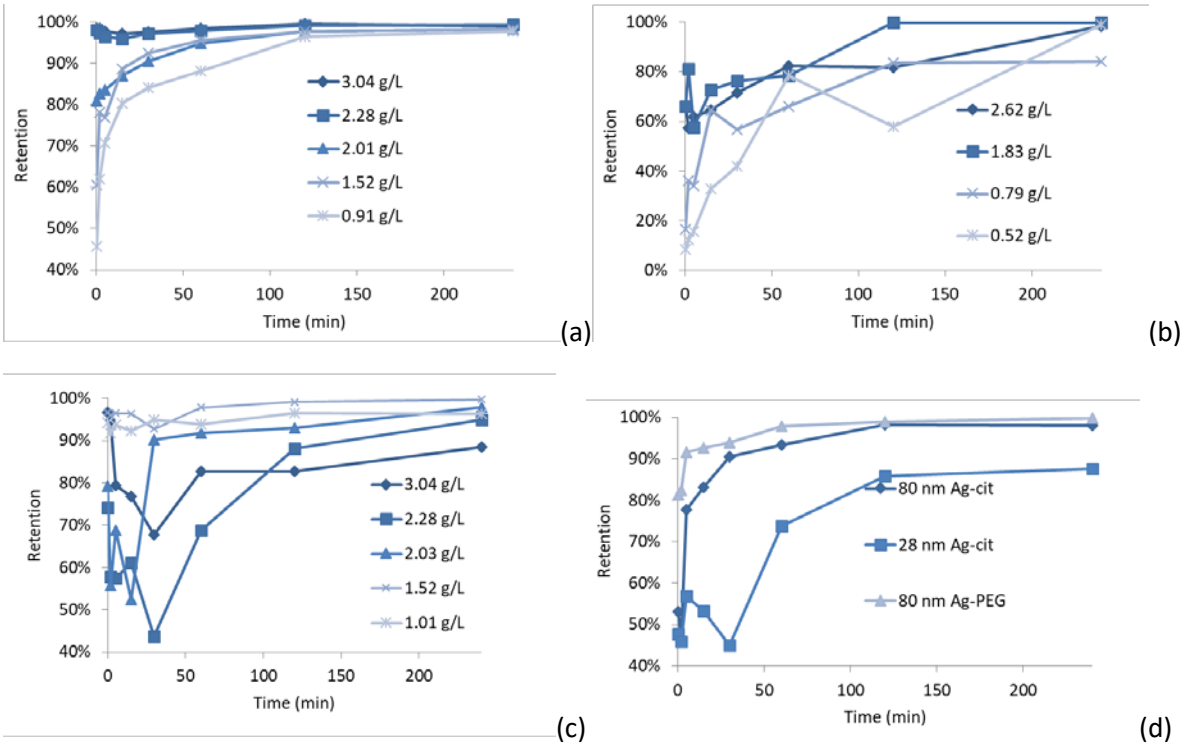

Figure S7. Retention as a function of time in all batch attachment experiments at different TSS concentrations at 200 rpm (a), 100 rpm (b), 25 rpm (c) or for different Ag NP at a TSS concentration of 3 g L-1 and 200 rpm stirring.

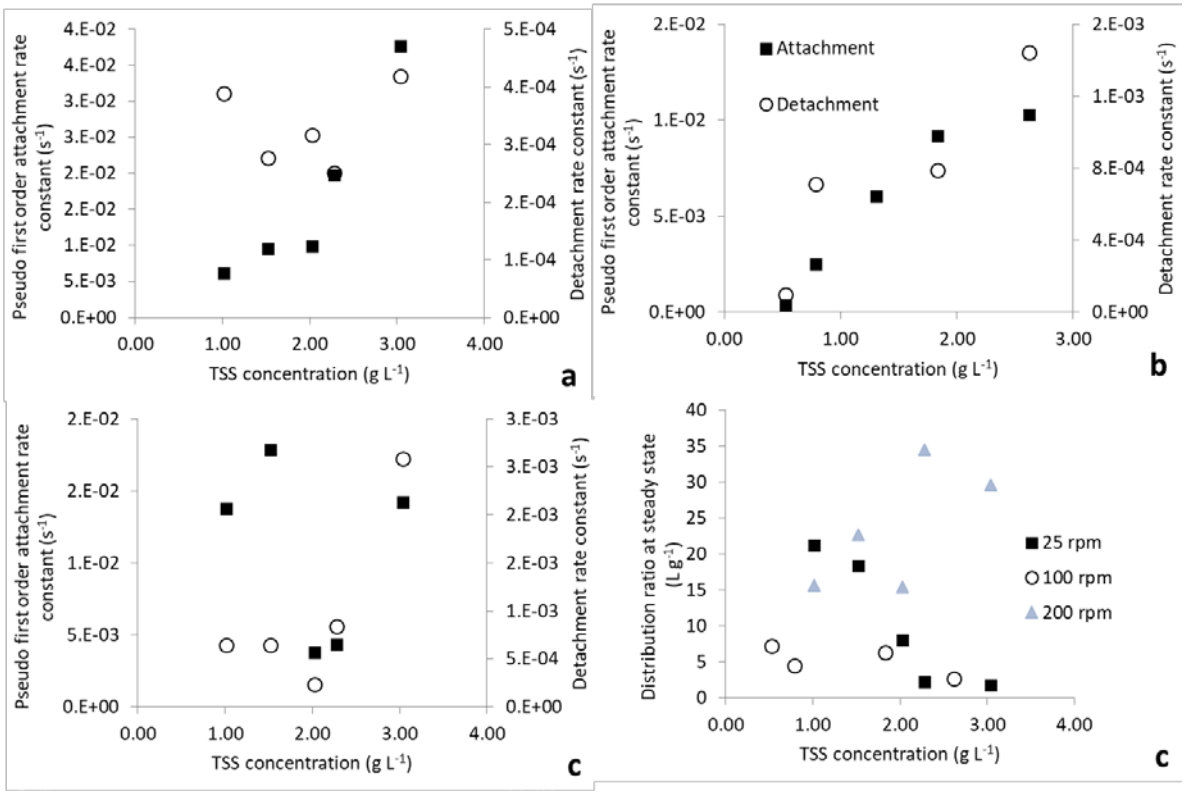

Figure S8. Pseudo first order attachment and detachment rate constants obtained for attachment experiments at 200 (a), 100 (b) and 25 (c) rpm stirring rates. (d) shows the distribution ratios obtained at these stirring rates.

Attachment and detachment rate calculation

Deduction of the following theory is largely based on Barton et al.[4], but is described in more detail here. Aggregation rates of particles can be calculated using Smoluchowski's law[5]:

$$\frac{dn_k}{dt} = \frac{1}{2}\sum_{i=1}^{k-1} k_{ij} n_i n_j - n_k \sum_{k=1}^{\infty} k_{ik} n_i \qquad Eq.\ 2$$

Where n_k is the suspended number concentration of ENP having size k, and n_i and n_j are the number concentrations of two particles whose aggregation leads to an aggregate with size k. k_{ij} and k_{ik} are the aggregation rate constants of the formation of aggregates with size k and of the further aggregation of such aggregates.

In studying the heteroaggregation of Ag NPs with AS, only the number concentration of NPs, n_{NP}, and the number concentration of AS particles, n_{AS}, are relevant. This implies that there is only one size class for both NPs and AS particles. In the case of NPs, it was verified that homoaggregation did not occur in ME (Figure S2). After a certain equilibration time, usually much less than 24 h[6], an equilibrium average floc size and number are established, the magnitude of which depends on the TSS concentration the shear rate and floc break up rate[7]. The ME is thus conceptualized as a suspension of uniform spheres having number concentration n_{AS}. The second term is to be removed in this conceptual model. AS particles do not aggregate further and the AS particle vastly outnumber the NP particles making attachment of one NP with one AS sludge the most likely process.

$$\frac{d(n_{AS-NP})}{dt} = -\frac{d(n_{NP})}{dt} = k_{att} n_P n_{AS} \qquad Eq.\ 3$$

k_{att} is the attachment rate constant of NPs attaching to AS particles. Eq. 3 expresses that the increase in the number of attached NPs should equal the reduction in the number of free NPs. The original formulation of Smoluchowski did not take detachment into account. Detachment is often considered having first-order kinetics with respect to attached particle number, a term that can be calculated as the difference between total number of NPs (n_t) and the number of free particles.

$$\frac{d(n_{NP})}{dt} = -k_{att} n_{NP} n_{AS} + k_{det}(n_t - n_{NP}) \qquad Eq.\ 4$$

Mass concentrations, rather than number concentrations were measured in this work. Particle number and mass concentration are related to each other by $n = CV_t/(\rho V_p)$, where C is the total mass of the particle, V_t the liquid volume, and ρ and V_p are the particle density and particle volume respectively. Such a relation can also be written for the conceptualized AS particles. Eq. 4 can therefore be rewritten in terms of mass concentration:

$$\frac{d\left(\frac{C_{NP}V_t}{\rho_{NP}V_{NP}}\right)}{dt} = -k_{att}\frac{C_{NP}V_t}{\rho_{NP}V_{NP}}\frac{C_{AS}V_t}{\rho_{AS}V_{AS}} + k_{det}\left(\frac{(C_t - C_{NP})V_t}{\rho_{NP}V_{NP}}\right) \qquad Eq.\ 5$$

where ρ_{NP} and ρ_{AS} are the particle (AS or ENP) densities and V_{NP} and V_{AS} the particle volumes. As homoaggregation does not occur, V_{NP} is time-independent, which means that eq. 5 can be simplified to eq. 6

$$\frac{dC_{NP}}{dt} = -\ k_{att}\ C_{NP}\ TSS + \ k_{det}\ (C_t - \ C_{NP}) \qquad Eq.\ 6$$

The term $TSS = C_{AS}V_t/(\rho_{AS}V_{AS})$ can be considered a constant, because the AS concentration is magnitudes higher than that of the Ag NP, resulting in equation 7, where $k'_{att} = k_{att} \times TSS$, the pseudo first order rate constant.

$$\frac{dC_{NP}}{dt} = -\ k'_{att}\ C_{NP} + \ k_{det}\ (C_t - \ C_{NP}) \qquad Eq.\ 7$$

This differential equation can be reformed into

$$\frac{dC_{NP}}{dt} + (k'_{att} + k_{det})C_{NP} = k_{det}C_t \qquad Eq.\ 8$$

This is a linear differential equation of the kind dy/dx + Py = Q where x = t, y = C_{NP}, P(t) = $k_{att} + k_{det}$ and Q(t) = $k_{det}C_t$. The integrating factor is

$$IF = exp\left(\int k'_{att} + k_{\mathrm{det}}dt\right) = exp\big((k'_{att} + k_{\mathrm{det}})t\big) + C$$

The solution to eq. 8 can then be found

$$C_{\mathrm{NP}} \times exp\big((k'_{att} + k_{\mathrm{det}})t\big) = \int k_{det}C_t exp\big((k'_{att} + k_{\mathrm{det}})t\big)dt + \mathrm{C}$$

$$C_{\mathrm{NP}} \times exp\big((k'_{att} + k_{det})t\big) = \frac{k_{det}C_t}{k'_{att} + k_{det}} \int exp\big((k'_{att} + k_{\mathrm{det}})t\big)d\big((k'_{att} + k_{\mathrm{det}})t\big) + \mathrm{C}$$

$$C_{\mathrm{NP}} \times exp\big((k'_{att} + k_{det})t\big) = \frac{k_{det}C_t}{k'_{att} + k_{det}} exp\big((k'_{att} + k_{\mathrm{det}})t\big) + \mathrm{C}$$

To find the unknown constant C, we use the fact that at t = 0, $C_{NP} = C_t$. The exponential factors equal 1, which implies that $C = C_t - k_{det}C_t/(k_{att}' + k_{det})$.

$$C_{\mathrm{NP}} \times exp\big((k'_{att} + k_{det})t\big) = \frac{k_{det}C_{\mathrm{t}}}{k'_{att} + k_{det}} exp\big((k'_{att} + k_{\mathrm{det}})t\big) + C_t - \frac{k_{det}C_t}{k'_{att} + k_{det}}$$

Rearranging gives:

$$C_{NP} = C_t exp(-(k'_{att} + k_{det})t) + \frac{k_{det}C_t}{k'_{att}+k_{det}}\big(1 - exp(-(k'_{att} + k_{det})t)\big) \qquad \textit{Eq. 9}$$

Eq. 9 has two unknown rate constants that can be found by non-linearly fitting the whole of eq. 9 to experimental data of C_{NP} as a function time. A simpler approach is to simplify eq. 6 by considering that detachment hardly occurs in the initial stages of the attachment experiments, because the attached concentration is near zero or $C_{NP} \approx C_t$. Removing the detachment term from eq. 6 results in a differential equation that easily solves into

$$C_{NP} = C_t exp(-k'_{att}t) \text{ or } ln\left(\frac{C_{NP}}{C_t}\right) = -k'_{att}t \qquad \textit{Eq. 10}$$

k_{att}' can thus be obtained from the slope of a ln-transformed curve of the first couple of measured C_{NP}/C_t values as a function of time. k_{att} can then be calculated from k_{att}'/TSS. At later times, detachment no longer is negligible. Eq. 9 converges, if t approaches infinity, to a constant value:

$$\frac{C_{NP}}{C_t} = \frac{k_{det}}{k'_{att}+k_{det}} \qquad \textit{Eq. 11}$$

Consider now the distribution ratio at steady state (X) which is defined as

$$X = \frac{C_t - C_{NP}}{C_{NP}C_{AS}} \qquad \textit{Eq. 12}$$

or, if written in terms of the observed average retention at steady state $R = 1 - C_{NP}/C_t$, we obtain the equation that is found in the main text.

$$X = \frac{\bar{R}}{(1-\bar{R})C_{AS}} \qquad \textit{Eq. 13}$$

Finally, combining eqs. 11 and 12 yields

$$k_{det} = \frac{k'_{att}}{XC_{AS}} \qquad \textit{Eq. 14}$$

Knowledge of k_{att} can thus lead to knowing k_{det} using eq. 11, provided that a constant, steady state value is reached within the experimental time.

Eqs. 10 and 14 were applied to all kinetic data. Figure S9 shows the ln-transformed data of Figure S7 (b), i.e. the retention data of the second batch ran at 200 rpm. The attachment rates were found by assuming zero attachment at time $t = 0$ and then applying eq. 10 using only the first two (nonzero) time points. Eq. 14 was then applied using the calculated k'_{att} and the distribution ratio calculated from the final data points, where it was assumed that steady state occurred.

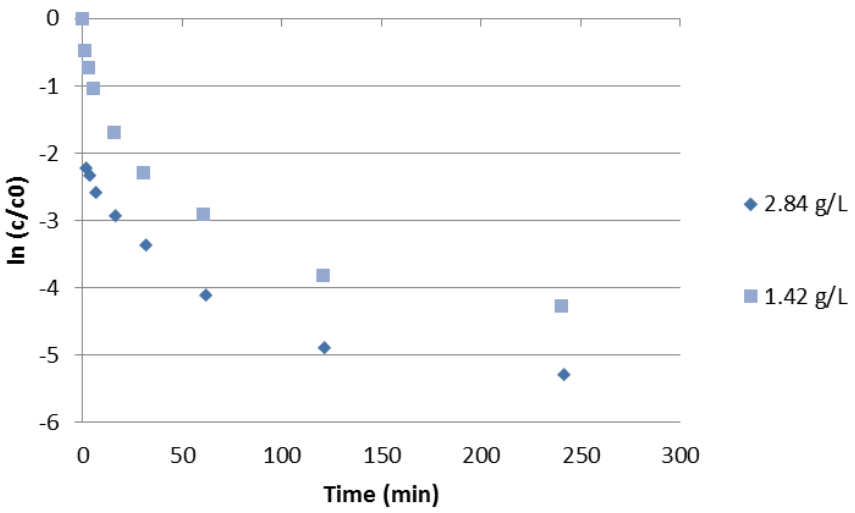

Figure S9 ln(CNP/Ct) for the batch experiment at 200 rpm done on a batch not shown in Figure S7 at two TSS concentrations (2.84 and 1.42 g/L).

Additional sedimentation experiments

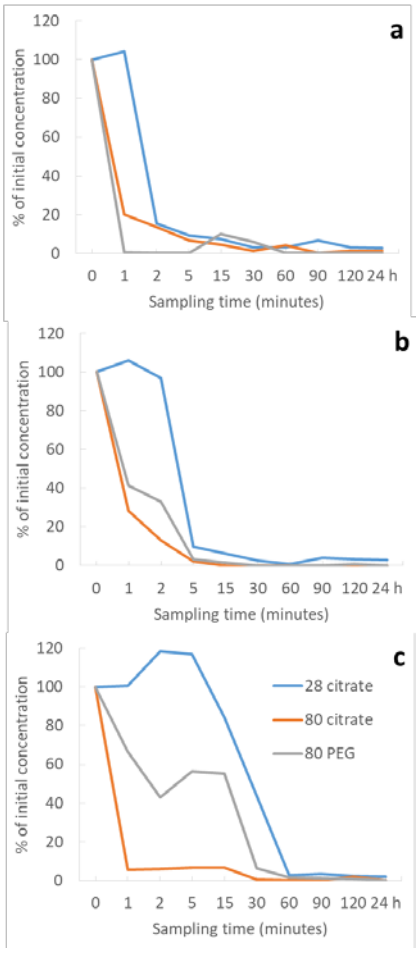

Figure S10. Second investigation of the time-dependent relative Ag mass concentration (% of initial concentration) of three different Ag ENP at a AS concentration of 1.4 g L-1 (a), 2.8 g L-1 (b), 5.6 g L-1 (c). Note that the time axis is not linear

Literature meta-analysis

Literature data

Table S3. Retention data and metadata sourced from the literature for the meta-analysis. Core is the material of the NM core. Coating is the nominal coating on the particle used in the listed studies. Size is the hydrodynamic diameter or nominal size whichever was available. Ct is the total nanomaterial mass concentration. [AS] is the activated sludge concentration. T_f is the time duration of the experiment where "steady state" indicates the experiment was done until a steady state concentration developed. "Artificial/real" indicates whether a sewage sample was created whereas "real" indicates that it was sampled from a local WWTP. "Type" indicates the scale of the study (batch, pilot plant, full scale). Separation indicates how suspended and attached NPs were distinguished. pH is the pH of the ME. Retention in the percentage of total remaining after the final duration of the experiment or at steady state. X is the distribution ratio (Calculation see main text) after the final duration of the experiment or at steady state.

Ref	Core	coating	Size (nm)	C_t (mg/L)	[AS] (g/L)	Tf (h)	artificial/ real	Type	separation	pH	Retention (%)	X
[8]	Ag	citrate	15.5	0.2	2.20	steady state	artificial	pilot plant	settling	7	89	3586
[8]	Ag	citrate	15.5	2	2.20	steady state	artificial	pilot plant	settling	7	0	N/A
[8]	Ag	GA	32.3	0.2	2.20	steady state	artificial	pilot plant	settling	7	94	6997
[8]	Ag	GA	32.3	2	2.20	steady state	artificial	pilot plant	settling	7	71	1102
[4]	Ag	GA	25	10	3.81	1	real	batch	settling	7.2	71	643
[4]	Ag	GA	25	50	3.81	1	real	batch	settling	7.2	73	702
[4]	Ag	GA	6	10	3.81	1	real	batch	settling	7.2	71	636
[4]	Ag	GA	6	50	3.81	1	real	batch	settling	7.2	65	492
[4]	Ag	PVP	40	10	3.81	1	real	batch	settling	7.2	95	4785
[4]	Ag	PVP	40	50	3.81	1	real	batch	settling	7.2	94	3971

[4]	Ag	PVP	8	10	3.81	1	real	batch	settling	7.2	88	1943
[4]	Ag	PVP	8	50	3.81	1	real	batch	settling	7.2	90	2261
[4]	CeO2	citrate	10	10	3.81	1	real	batch	settling	7.2	86	1667
[4]	CeO2	citrate	10	50	3.81	1	real	batch	settling	7.2	83	1319
[4]	CeO2	none	8	10	3.81	1	real	batch	settling	7.2	91	2590
[4]	CeO2	none	8	50	3.81	1	real	batch	settling	7.2	99	21610
[4]	TiO2	none	20	10	3.81	1	real	batch	settling	7.2	95	5094
[4]	TiO2	none	20	50	3.81	1	real	batch	settling	7.2	99	23598
[4]	ZnO	none	30	10	3.81	1	real	batch	settling	7.2	91	2720
[4]	ZnO	none	30	50	3.81	1	real	batch	settling	7.2	94	4263
[9]	CeO2	citrate	10	1.5	10.00	steady state	artificial	pilot plant	centrifugation	N/A	98	5456
[9]	CeO2	none	8	1.5	10.00	steady state	artificial	pilot plant	centrifugation	N/A	98	6422
[10]	CeO2	citrate	10	1.5	3.00	1	real	batch	settling	N/A	90	3000
[10]	CeO2	citrate	10	1.5	0.92	1	real	batch	settling	N/A	48	1000
[10]	CeO2	none	8	1.5	1.92	1	real	batch	settling	N/A	92	6000
[10]	CeO2	none	8	1.5	0.36	1	real	batch	settling	N/A	52	3000
[11]	Ag	PVP	40	500	4.50	120	real	pilot plant	settling	6.7	99	22000
[12]	Cu	none	125	1.8	0.65	20	real	batch	0.45 um filtration	7.6	94	22500
[12]	Cu	none	125	3.5	0.65	20	real	batch	0.45 um filtration	7.6	95	26434

[12]	Cu	none	125	5.3	0.65	20	real	batch	0.45 um filtration	7.6	95	29231
[12]	Cu	none	125	7.0	0.65	20	real	batch	0.45 um filtration	7.6	96	33427
[12]	Cu	none	125	8.8	0.65	20	real	batch	0.45 um filtration	7.6	96	37909
[13]	TiO2	none	21	1	1.80	steady state	artificial	pilot plant	settling	7.3	96	12297
[13]	TiO2	none	21	5	1.30	steady state	artificial	pilot plant	settling	7.3	98	35588
[13]	TiO2	none	21	10	3.00	steady state	artificial	pilot plant	settling	7.2	96	7859
[14]	CeO2	none	50	68	3.50	15.2	real	batch	settling	7.4	94	4727
[14]	CeO2	none	50	55	3.50	15.2	real	pilot plant	settling	7.4	97	8118
[15]	Ag	none	20	1	1.20	3	artificial	batch	settling	7.5	67	1692
[15]	Ag	none	20	4	1.20	3	artificial	batch	settling	7.5	58	1151
[15]	Ag	none	20	8	1.20	3	artificial	batch	settling	7.5	73	2253
[15]	Ag	none	20	12	1.20	3	artificial	batch	settling	7.5	41	584
[16]	Ag	tween20	3	0.17	2.50	steady state	real	pilot plant	settling	6.5	80	1600
[16]	Ag	tween20	3	0.17	3.50	steady state	real	pilot plant	settling	6.5	99	28286
[17]	Ag	citrate	10	25	3.45	24	real	batch	centrifugation		69	645
[17]	Ag	GA	6	25	3.45	24	real	batch	centrifugation		42	210
[17]	Ag	none	30	25	3.45	24	real	batch	centrifugation		91	2895
[17]	Ag	PVP	10	25	3.45	24	real	batch	centrifugation		91	3004

[18]	Ag	citrate	23	1	0.27	0.5		batch	settling	7.3	6	236
[18]	Ag	citrate	23	1	0.73	0.5		batch	settling	7.3	10	152
[18]	Ag	citrate	23	0.1	2.40	10		batch	settling	7.3	100	416250
[18]	Ag	citrate	23	10	2.40	10		batch	settling	7.3	100	416250
[19]	SiO2	none	56	2470	0.29	1.5		batch	centrifugation	7.18	0	N/A
[19]	SiO2	tween20	56	2470	0.29	1.5		batch	centrifugation	7.18	75	10239
[20]	Ag	polyoxyethylene fatty acid ester	60	2.4	3.00	steady state	real	pilot plant	0.7 um filtration	7.4	86	2100
[20]	Ag	polyoxyethylene fatty acid ester	60	0.13	3.00	steady state	real	pilot plant	0.7 um filtration	7.4	97	10778
[21]	TiO2	none	40	843	0.34	steady state	real	full plant	settling	7.2	96	70816
[21]	TiO2	none	40	99	0.10	steady state	real	full plant	settling	7.2	33	5155
[21]	TiO2	none	40	2572	2.22	steady state	real	full plant	settling	7.2	99	82304
[21]	TiO2	none	40	35	0.01	steady state	real	full plant	settling	7.2	0	N/A
[21]	TiO2	none	40	36	0.01	steady state	real	full plant	settling	7.2	44	133333
[22]	Ag	carboxyl	3	0.5	0.05	3	real	batch	settling	7	96	480000
[22]	Ag	carboxyl	3	0.5	0.40	3	real	batch	settling	7	97	80833
[22]	Ag	none	13	0.6	0.05	3	real	batch	settling	7	18	4390
[22]	Ag	none	13	0.6	0.40	3	real	batch	settling	7	40	1667
[22]	C60	none	88	4	0.05	3	real	batch	settling	7	78	70909
[22]	C60	none	88	4	0.40	3	real	batch	settling	7	88	18333

[22]	C60	none	88	3	0.05	3	real	batch	settling	7	35	10769
[22]	C60	none	88	3	0.20	3	real	batch	settling	7	80	20000
[22]	C60	none	88	3	0.40	3	real	batch	settling	7	82	11389
[22]	C60	PVP	100	2	0.05	3	real	batch	settling	7	7	1505
[22]	C60	toluene	56	3	0.05	3	real	batch	settling	7	17	4096
[22]	C60	toluene	56	3	0.20	3	real	batch	settling	7	60	7500
[22]	C60	toluene	56	3	0.40	3	real	batch	settling	7	81	10658
[22]	fullerol	none	48	12	0.05	3	real	batch	settling	7	0	
[22]	fullerol	none	48	12	0.40	3	real	batch	settling	7	12	341
[22]	fullerol	none	48	14	0.05	3	real	batch	settling	7	7	1505
[22]	fullerol	none	48	14	0.20	3	real	batch	settling	7	27	1849
[22]	fullerol	none	48	14	0.40	3	real	batch	settling	7	44	1964
[22]	SiO2	isothiocyanate	85	2.1	2.00	3	real	batch	settling	7	96	10688
[22]	SiO2	isothiocyanate	85	11	2.00	3	real	batch	settling	7	93	6551
[22]	SiO2	isothiocyanate	85	21	2.00	3	real	batch	settling	7	93	7126
[22]	SiO2	isothiocyanate	85	42	2.00	3	real	batch	settling	7	95	9251
[22]	SiO2	isothiocyanate	85	105	2.00	3	real	batch	settling	7	92	6107
[22]	TiO2	none	40	0.83	0.05	3	real	batch	settling	7	2	408
[22]	TiO2	none	40	0.83	0.40	3	real	batch	settling	7	22	705
[23]	Ag	carboxyl	2	2.1	0.80	3		batch	settling		60	1899

[23]	Ag	carboxyl	2	2	0.80	3		batch	settling		75	3750
[23]	Ag	citrate	2.4	0.4	0.80	3		batch	settling		39	789
[23]	Ag	GA	34	0.5	0.80	3		batch	settling		62	2066
[23]	Ag	PVP	8.8	0.1	0.80	3		batch	settling		48	1168
[23]	Au	PVP	10	0.9	0.80	3		batch	settling		55	1515
[23]	Au	Tannic acid	7.1	2.2	0.80	3		batch	settling		92	15197
[23]	C60	none	35.5	3.4	0.80	3		batch	settling		95	23260
[23]	Polystyrene	carboxyl	35	2	0.80	3		batch	settling		93	17689
[23]	Polystyrene	sulfate	13	2	0.80	3		batch	settling		94	21071
[24]	CeO2	none	24.5	100	2.00	steady state	artificial	pilot plant	centrifugation		94	7833
[25]	ZnO	caprylic triglyceride	39	N/A	N/A	steady state	real	pilot plant	settling	6.8		
[25]	ZnO	none	39	N/A	N/A	steady state	real	pilot plant	settling	6.7		
[25]	ZnO	none	35	N/A	N/A	steady state	real	pilot plant	settling	6.8		
[26]	Ag	citrate	10	0.72	12.69	steady state	real	pilot plant	settling	6.7	85	436
[26]	Ag	mercaptosuccinic acid	9	0.78	12.69	steady state	real	pilot plant	settling	6.8	83	392
[26]	Ag	PVS	6	0.78	12.69	steady state	real	pilot plant	settling	6.8	86	482
[26]	AgCl	PVP	200	0.72	12.69	steady state	real	pilot plant	settling	6.7	86	490

[27]	Ag	PVP	52	N/A		steady state	real	pilot plant	settling	6.4	99	
[27]	ZnO	none	10	N/A		steady state	real	pilot plant	settling	6.4	92	
[28]	ZnO	SDBS	140	205	20.50	N/A	artificial	batch	settling	6.9	100	16080
[28]	ZnO	SDBS	140	1025	20.50	N/A	artificial	batch	settling	6.9	100	15336
[28]	ZnO	SDBS	140	2050	20.50	N/A	artificial	batch	settling	6.9	99	9297
[28]	ZnO	SDBS	140	4100	20.50	N/A	artificial	batch	settling	6.9	99	7825
[29]	CeO2	none	25	1		N/A	real	pilot plant	settling	N/A	96	
[30]	Ag	ethylene glycol	41	0.5	2	6	real	batch	settling	7.5	93	6167
[30]	Ag	ethylene glycol	41	5	2	6	real	batch	settling	7.5	94	7437
[30]	Ag	ethylene glycol	41	10	2	6	real	batch	settling	7.5	92	5910
[31]	Ag	carboxyl	5	0.6	1.8	steady state	real	pilot plant	0.7 um filtration	7	88	4074
[31]	Ag	carboxyl	5	0.6	1.1	steady state	real	pilot plant	0.7 um filtration	7	49	873
[31]	Ag	carboxyl	5	2	0.55	steady state	real	pilot plant	0.7 um filtration	7	58	2511
[31]	C60	none	88	0.76	2	steady state	real	pilot plant	0.7 um filtration	7	96	12000
[31]	C60	none	88	0.76	0.6	steady state	real	pilot plant	0.7 um filtration	7	92	19167
[31]	C60	none	88	0.07	0.6	steady state	real	pilot plant	0.7 um filtration	7	97	53889
[31]	C60	none	88	2	0.6	steady state	real	pilot plant	0.7 um filtration	7	83	8137

[31]	fullerol	none	40	2	0.6	steady state	real	pilot plant	0.7 um filtration	7	75	5000
[31]	TiO2	none	20	2	1.3	steady state	real	pilot plant	0.7 um filtration	7	97	24872
[32]	TiO2	unkown	N/A	0.62	N/A	steady state	real	full plant	settling	N/A	99	
[32]	TiO2	unkown	N/A	0.18	N/A	steady state	real	full plant	settling	N/A	96	
[32]	TiO2	unkown	N/A	0.36	N/A	steady state	real	full plant	settling	N/A	99	
[32]	TiO2	unkown	N/A	0.14	N/A	steady state	real	full plant	settling	N/A	99	
[32]	TiO2	unkown	N/A	0.58	N/A	steady state	real	full plant	settling	N/A	97	
[32]	TiO2	unkown	N/A	0.23	N/A	steady state	real	full plant	settling	N/A	99	
[32]	TiO2	unkown	N/A	0.55	N/A	steady state	real	full plant	settling	N/A	98	
[32]	TiO2	unkown	N/A	0.31	N/A	steady state	real	full plant	settling	N/A	100	
[32]	TiO2	unkown	N/A	0.42	N/A	steady state	real	full plant	settling	N/A	99	
[33]	Ag	PVA	29	40	3.03	3		batch	0.45 um filtration	7.5	91	3144
[33]	Ag	PVA	29	40	3.03	72		batch	0.45 um filtration	7.5	97	9449
[33]	Ag	PVA	29	40	3.03	336		batch	0.45 um filtration	7.5	99	27758

Additional ENP properties

Table S4. Particle properties used for literature meta-analysis.

Core material	Density (g cm^{-3})	Hamaker constant (J)
Ag	10.2	3.354E-20
C60	1.65	7.76E-20
TiO2	4.23	4.30E-20
Fe	7.87	5.38E-20
SWCNT	0.11	6.2478E-19
ZnO	5.61	1.90E-20
Cu	8.96	1.75E-19
MWCNT	1.75	6.85E-20
fullerol	1.2	4.94E-19
SiO2	2.65	6.35E-20
alumoxane	1.3	1.50E-19
FeOOH	3.8	2.29E-20
polystyrene	1.05	9.80E-20
CdTe	6.2	1.10E-19
CdSe	5.82	1.10E-19
montmorillonite	2.63	5.00E-20
HAP	2.3	1.30E-20
Fe3O4	5.15	4.30E-20
CeO2	7.65	5.57E-20
Au	19.3	1.00E-20

Table S5. Coating properties and molecular weights (MW g mol-1) used for literature meta-analysis.

Molecule	Full name	Min MW	Max MW	Average
GA	Gum arabic	380000	850000	615000
PVA	Polyvinylalcohol	26300	30000	28150
PVP	Polyvinylpyrollidone	10000	360000	185000
SDBS	Sodium dodecyl benzeoate	3485	3485	3485
THF	Tetrahydrofuran	72	72	72
tannic acid		1701	1701	1701
acetic acid		60	60	60
caprylic triglyceride		5330	5330	5330
”carboxyl”		unknown		
carboxymethylcellulose		250000	700000	475000
cetyltrimethylammonium-bromide		364	364	364
citrate		214	214	214
ethylene glycol		200	3400	1800
humic acid		2000	20000	11000
isothiocyanate		59	59	59
mercaptosuccinic acid		150	150	150
polyacrilic acid		1600	10000	5800
polyaspartate		2000	11000	6500
sulfate		96	96	96
toluene		92.14	92.14	92.14
triblock		125000	125000	125000
tween20		1227	1227	1227

Results

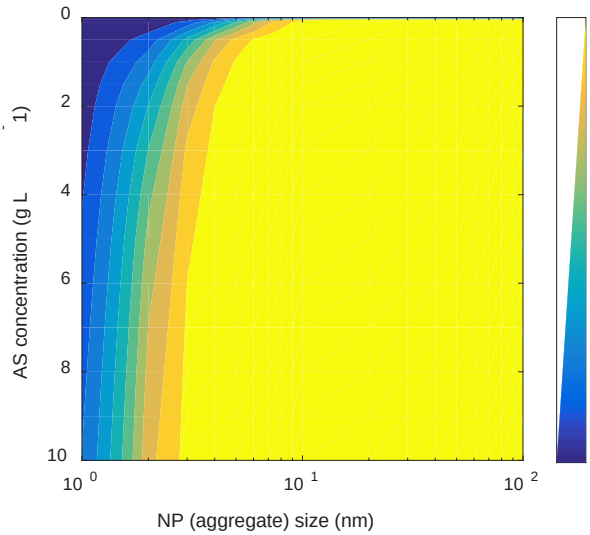

Figure S11. Predicted retention by AS as a function of NP (aggregate) diameter and AS concentration based on equationss. 2 and 4 found in the main text.

References

1. A. Sochan, C. Polakowski and G. Lagod, *Ecological Chemistry and Engineering S-Chemia I Inzynieria Ekologiczna S*, 2014, **21**, 137-145.
2. M. Elimech, J. Gregory, X. Jia and R. A. Williams, *Particle Deposition and Aggregation Measurement, Modelling and Simulation*, Butterworth Heineman. 1995.
3. Gryaab AB. 2013.
4. L. E. Barton, M. Therezien, M. Auffan, J. Y. Bottero and M. R. Wiesner, *Environ. Eng. Sci.*, 2014, **31**, 421-427.
5. M. Smoluchowski, *Physik. Chem*, 1917, **92**.
6. F. Mietta, C. Chassagne and J. C. Winterwerp, *Journal of Colloid and Interface Science*, 2009, **336**, 134-141.
7. P. T. Spicer and S. E. Pratsinis, *AIChE Journal*, 1996, **42**, 1612-1620.
8. C. L. Alito and C. K. Gunsch, *Environ. Sci. Technol.*, 2014, **48**, 970-976.
9. L. E. Barton, M. Auffan, M. Bertrand, M. Barakat, C. Santaella, A. Masion, D. Borschneck, L. Olivi, N. Roche, M. R. Wiesner and J. Y. Bottero, *Environmental Science and Technology*, 2014, **48**, 7289-7296.
10. L. E. Barton, M. Auffan, L. Olivi, J.-Y. Bottero and M. R. Wiesner, *Environmental Pollution*, 2015, **203**, 122-129.
11. C. L. Doolette, M. J. McLaughlin, J. K. Kirby, D. J. Batstone, H. H. Harris, H. Ge and G. Cornelis, *Chemistry Central Journal*, 2013, **7**.
12. R. Ganesh, J. Smeraldi, T. Hosseini, L. Khatib, B. H. Olson and D. Rosso, *Environmental Science & Technology*, 2010, **44**, 7808-7813.
13. S. Gartiser, F. Flach, C. Nickel, M. Stintz, S. Damme, A. Schaeffer, L. Erdinger and T. A. J. Kuhlbusch, *Chemosphere*, 2014, **104**, 197-204.
14. F. Gómez-Rivera, J. A. Field, D. Brown and R. Sierra-Alvarez, *Bioresource Technology*, 2012, **108**, 300-304.
15. L. Gu, Q. Li, X. Quan, Y. Cen and X. Jiang, *Water Research*, 2014, **58**, 62-70.
16. J. Hedberg, C. Baresel and I. Odnevall Wallinder, *Journal of Environmental Science and Health, Part A*, 2014, **49**, 1416-1424.
17. C. O. Hendren, A. R. Badireddy, E. Casman and M. R. Wiesner, *Science of The Total Environment*, 2013, **449**, 418-425.
18. L. Hou, K. Li, Y. Ding, Y. Li, J. Chen, X. Wu and X. Li, *Chemosphere*, 2012, **87**, 248-252.
19. H. P. Jarvie, H. Al-Obaidi, S. M. King, M. J. Bowes, M. J. Lawrence, A. F. Drake, M. A. Green and P. J. Dobson, *Environmental Science & Technology*, 2009, **43**, 8622-8628.
20. R. Kaegi, A. Voegelin, B. Sinnet, S. Zuleeg, H. Hagendorfer, M. Burkhardt and H. Siegrist, *Environmental Science & Technology*, 2011, **45**, 3902-3908.
21. M. A. Kiser, P. Westerhoff, T. Benn, Y. Wang, J. Perez-Rivera and K. Hristovski, *Environmental Science & Technology*, 2009, **43**, 6757-6763.
22. M. A. Kiser, H. Ryu, H. Jang, K. Hristovski and P. Westerhoff, *Water Research*, 2010, **44**, 4105-4114.
23. M. A. Kiser, D. Ladner, K. D. Hristovski and P. Westerhoff, *Environ. Sci. Tech.*, 2012.
24. L. K. Limbach, R. Bereiter, E. Mueller, R. Krebs, R. Gaelli and W. J. Stark, *Environmental Science & Technology*, 2008, **42**, 5828-5833.
25. E. Lombi, E. Donner, E. Tavakkoli, T. W. Turney, R. Naidu, B. W. Miller and K. G. Scheckel, *Environ. Sci. Tech.*, 2012, **46**, 9089-9096.
26. E. Lombi, E. Donner, S. Taheri, E. Tavakkoli, Å. K. Jämting, S. McClure, R. Naidu, B. W. Miller, K. G. Scheckel and K. Vasilev, *Environ. Pollut.*, 2013, **176**, 193-197.
27. R. Ma, C. Levard, J. D. Judy, J. M. Unrine, M. Durenkamp, B. Martin, B. Jefferson and G. V. Lowry, *Environmental Science & Technology*, 2014, **48**, 104-112.
28. H. Mu, X. Zheng, Y. Chen, H. Chen and K. Liu, *Environmental Science & Technology*, 2012, **46**, 5997-6003.

29. G. Qiu, S.-Y. Neo and Y.-P. Ting, *Water Science and Technology*, 2016, **73**, 95-101.
30. K. Tiede, A. B. A. Boxall, X. M. Wang, D. Gore, D. Tiede, M. Baxter, H. David, S. P. Tear and J. Lewis, *Journal of Analytical Atomic Spectrometry*, 2010, **25**, 1149-1154.
31. Y. F. Wang, P. Westerhoff and K. D. Hristovski, *J. Hazard. Mater.*, 2012, **201**, 16-22.
32. P. Westerhoff, G. Song, K. Hristovski and M. A. Kiser, *Journal of Environmental Monitoring*, 2011, **13**, 1195-1203.
33. Y. Yang, Q. Chen, J. D. Wall and Z. Hu, *Water Research*, 2012, **46**, 1176-1184.